



UK Centre for
Ecology & Hydrology

CCRA3 flooding projections Task 2a: High resolution climate change projections—Fluvial

Technical Note

Kay AL, Stewart EJ, Davies HN, Rudd AC, Vesuviano G

With support from

Paul Sayers, Sayers and Partners

Client Ref: CCRA3 Floods Task 2a

Issue Number 1.1

Date: March 2020

Title CCRA3 flooding projections Task 2a: High resolution climate change projections—Fluvial

Client Sayers & Partners Ltd

Client reference CCRA3 Floods Task 2a

Confidentiality, copyright and reproduction [add statement here as required]

UKCEH reference NEC07063/ Issue number 1.2

UKCEH contact details UK Centre for Ecology & Hydrology
Maclean Building
Benson Lane
Wallingford
Oxon
OX10 8BB

t: +44 (0)1491 692392
e: alkay@ceh.ac.uk

Author Kay, Alison

Approved by Nick Reynard

Date March 2020

Executive Summary

As part of the CCRA3 flooding projections project, this task provides

1. Estimates of percentage changes in flood peaks for locations across the UK, using UKCP18 probabilistic projections applied for a set of global mean surface temperature (GMST) changes (ranging from 1.0°C to 4.5°C in increments of 0.5°C).
2. Estimates of change in return period corresponding to a range of peak flow uplifts, as look-up tables, for locations across the UK.

The data are provided for use within the Future Flood Explorer (FFE) to investigate potential future flood risks under climate change, under a range of adaptation options.

This technical report details the methodology used to produce the flood peak and return period data, including differences in the methods used for Great Britain and Northern Ireland.

Contents

1	Introduction.....	1
2	Percentage changes in flood peaks	1
2.1	Background.....	1
2.2	GMST changes and time-slice selection	3
2.3	Precipitation changes	7
2.4	Flood peak changes for Great Britain	11
2.5	Flood peak changes for Northern Ireland	14
2.6	Correction of bias in impacts derived from incomplete ensembles	16
2.7	Uncertainty from emissions trajectory	22
2.8	Additional information	24
3	Changes in return periods.....	24
3.1	Mapping 1km river cells to 50m pixels	24
3.2	Return period analysis for 50m pixels	25
4	References	30

1 Introduction

As part of the CCRA3 flooding projections project, this task provides

1. Estimates of percentage changes in flood peaks for locations across the UK, using UKCP18 probabilistic projections applied for a set of global mean surface temperature (GMST) changes (ranging from 1.0°C to 4.5°C in increments of 0.5°C).
2. Estimates of change in return period corresponding to a range of peak flow uplifts, as look-up tables, for locations across the UK.

The data are used within the Future Flood Explorer (FFE) to investigate potential future flood risks under climate change, under a range of adaptation options. The decoupling of return period changes from estimated flood peak changes allows adaptation options to be applied more freely.

2 Percentage changes in flood peaks

2.1 Background

To provide percentage changes in flood peaks, this task builds upon CEH's work for the EA-funded project "Providing more locally-appropriate information on potential impacts of climate change on flood peaks in England and Wales", which also had some funding from SEPA to extend coverage to Scotland. That project built upon previous projects FD2020 (Reynard et al. 2009) and FD2648 (Kay et al. 2011), which

- developed a sensitivity framework for estimating the response of catchment flood peaks to climatic changes (Prudhomme et al. 2010);
- derived a set of response types, and corresponding representative (average) flood response surfaces, representing the sensitivity of catchments across Great Britain (GB) to climatic changes (Prudhomme et al. 2013 and Figure 2.1); and
- applied the average flood response surfaces with the UKCP09 probabilistic projections, to assess the potential range of impacts of climate change on flood peaks on a regional basis, for river-basin regions across Great Britain (Kay et al. 2014a,b).

The most recent EA project (Kay et al. 2020) used the sensitivity framework approach but with a national-scale grid-based hydrological model (Grid-to-Grid; Bell et al. 2009) to enable a consistent assessment of sensitivity for catchments across GB (gauged or ungauged). It then applied the UKCP18 probabilistic projections for river-basin regions (Met Office Hadley Centre 2018) by overlaying them on the modelled response surfaces for grid boxes across GB, to assess the potential range of impacts of climate change on flood peaks on a 1km grid (for 1km cells with catchment area $\geq 100\text{km}^2$, hereafter termed 1km river cells). The output of the EA project will be made available via a web-tool, for three 30-year time-slices (2020s, 2050s, 2080s) and four emissions scenarios (RCP2.6, RCP4.5, RCP6.0, RCP8.5). Figure 2.2 shows the UKCP18 river-basin regions, along with the number of 1km river cells in each region, to illustrate the scale of information now available (12,421 1km river cells across GB), compared to just regional values previously (19 regions across GB). Note that no data are provided for 1km cells considered as tidal.

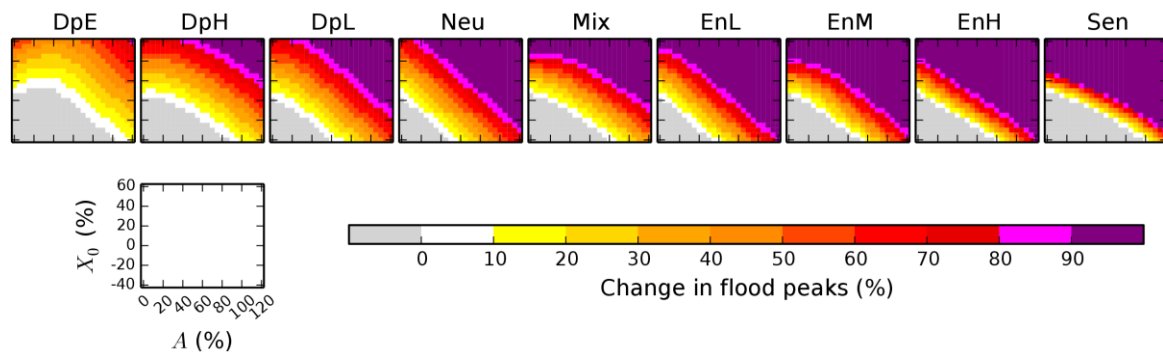


Figure 2.1 Representative flood response surfaces corresponding to each of the nine flood response types of FD2020 (Damped-Extreme, Damped-High, Damped-Low, Neutral, Mixed, Enhanced-Low, Enhanced-Medium, Enhanced-High, Sensitive; left to right), for changes in 50-year return period flood peaks (see colour key, bottom-right). The sensitivity domain of changes in precipitation (see key, bottom-left) is defined by the harmonic mean X_0 (y-axis) and amplitude A (x-axis) via $X(t) = X_0 + A \cos[2\pi(t - 1)/12]$ for month t (January = 1), using 5% intervals for both X_0 and A (Prudhomme et al. 2010). The response surface for the Neutral response type shows flood peak changes similar to the precipitation changes, while Damped types show flood peak changes generally smaller than the precipitation changes, and Enhanced types show flood peak changes that are often larger than the precipitation changes. Flood peak changes for the Mixed and Sensitive types are more dependent on the specific seasonality and magnitude of precipitation changes.

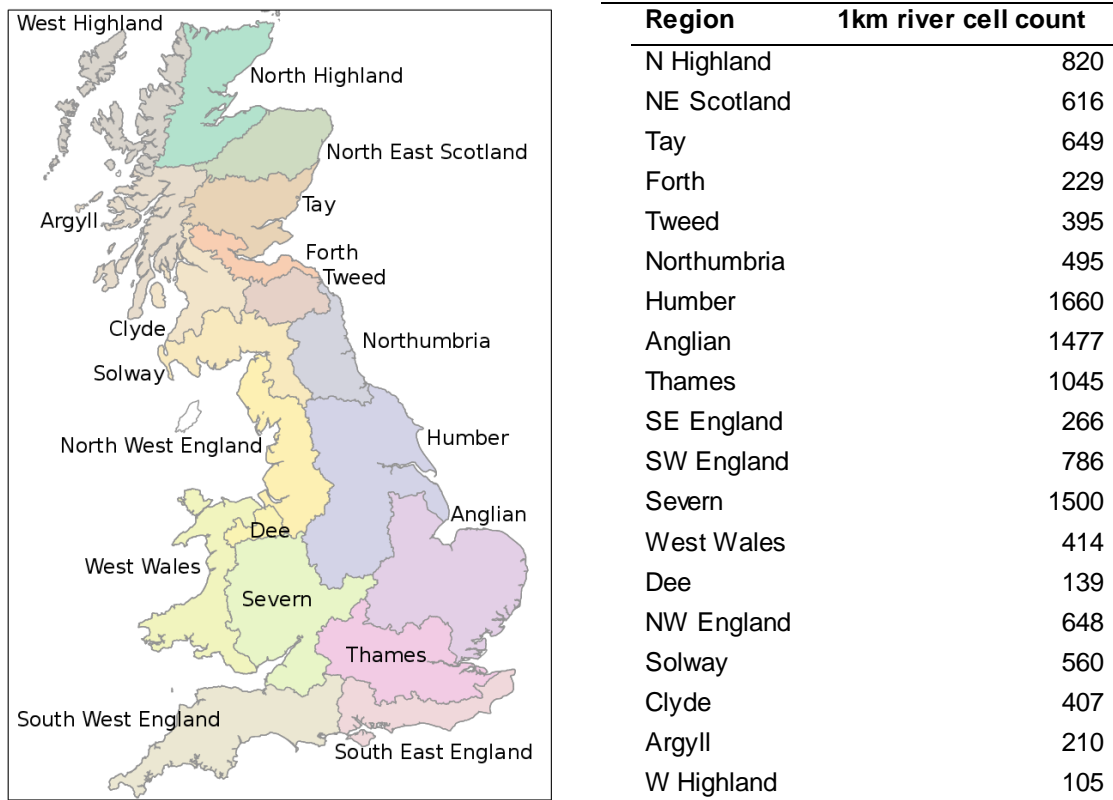


Figure 2.2 The UKCP18 river-basin regions covering GB (excluding Orkney/Shetland), and the number of 1km river cells (catchment area $\geq 100\text{km}^2$) located in each region, for which changes in flood peaks can be derived. There are a total of 12,421 1km river cells, across 19 river-basin regions.

Here, the FFE analysis required information on flood changes corresponding to a range of GMST changes with relatively small graduations (including, but not limited to 2°C and 4°C increases from a pre-industrial period). This was achieved by extending the sets of UKCP18 projection data overlaid on the response surfaces produced by the EA project. New sets of river-basin region projections were derived for each of the required GMST changes, by selecting, for each ensemble member, the 20-year time-slice with a GMST change most closely matching the required GMST change. This type of approach is typically termed ‘time-sampling’ (James et al. 2017). Details are provided below.

2.2 GMST changes and time-slice selection

Files of yearly GMST anomalies (Dec 1859–Nov 2099) corresponding to the UKCP18 probabilistic projections are obtained from the UKCP18 CEDA archive (Met Office Hadley Centre 2018). There are 3,000 projections for each of the four RCPs, and the anomalies are in °C relative to a baseline of 1981-2000. The range of the GMST anomalies for each RCP is shown in Figure 2.3. The data for RCP8.5 are used for all of the required GMST changes, as this high RCP is the one covering the greatest range of GMST changes. Data for the other RCPs (RCP2.6, RCP4.5 and RCP6.0) are only used for a GMST change of 1.5°C, to test the effect of the emissions trajectory choice on the results (Section 2.7).

The yearly GMST anomalies are turned into time-slice mean changes for all possible future 20-year time-slices (1971-1990, 1972-1991, ... , 2080-2099) from an alternative (pre-industrial) baseline (1860-1900) [See Box 1, page 6]. These time-slice mean GMST changes are shown in Figure 2.4.

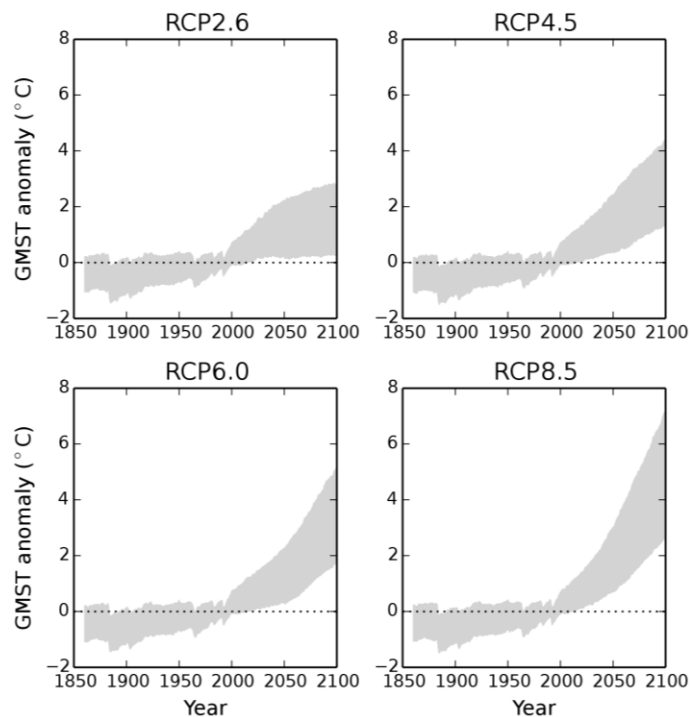


Figure 2.3 Yearly GMST anomalies (°C) for each RCP, relative to 1981-2000 baseline.

For each required GMST change and each ensemble member, the time-slice with mean GMST change closest to the required GMST change is identified (within a

maximum deviation of 0.04999°C). Table 2.1 shows an example of this time-slice selection for a subset of 7 ensemble members. Figure 2.5 summarizes the number of times each 20-year time-slice is selected for each required GMST change.

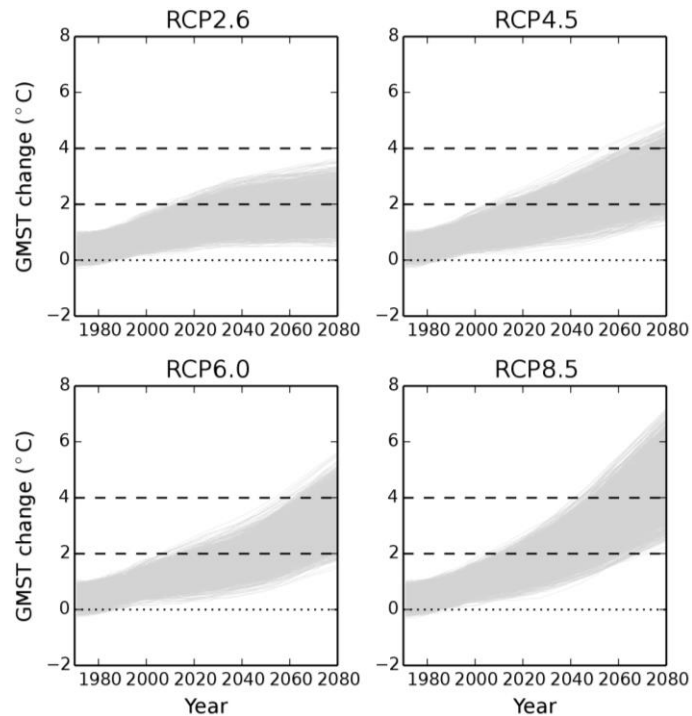


Figure 2.4 Time-slice mean GMST changes (°C) for each RCP, relative to pre-industrial period (1860-1900). 2°C and 4°C GMST change thresholds are shown by dashed lines; no ensemble members reach 4°C for RCP2.6.

Note that not all required GMST changes have a full set of 3,000 samples (Table 2.2), as not all ensemble members reach each required GMST change (Figure 2.4). For this reason, the analysis could not go beyond a 4.5°C GMST change, since over 50% of the 3000 ensemble members are missing for higher GMST changes (e.g. 67% are missing for a 5.0°C GMST change, and nearly 93% are missing for a 6.0°C GMST change; Table 2.2). Even for the GMST changes included, for those with incomplete ensembles (3.0°C and above) there is some bias in the corresponding sets of precipitation changes (Section 2.3) and thus in the derived flood peak changes, which needs to be accounted for (Section 2.6).

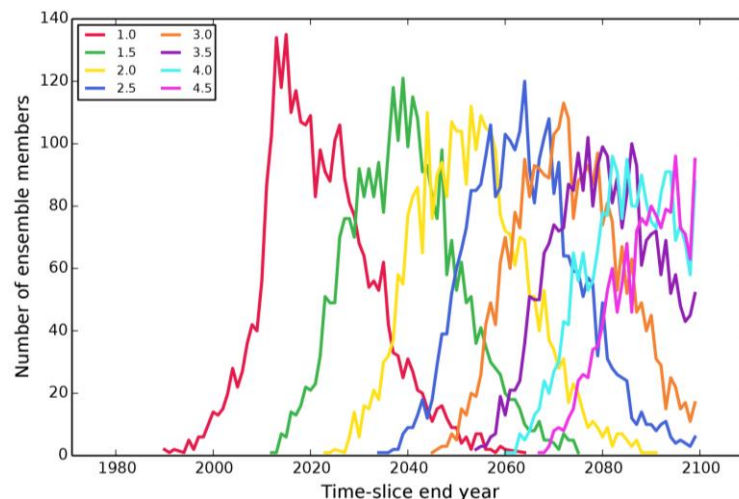


Figure 2.5 Summary plot showing, for each required GMST change, the number of ensemble members for each 20-year time-slice (RCP8.5).

Table 2.1 Example showing selection of 20-year time-slices corresponding to a 1°C GMST change (highlighted in yellow), for a subset of 7 ensemble members (RCP 8.5). Note that not all 20-year time-slices are shown; there are both earlier and later time-slices available.

20-year time-slice	Ensemble member						
	0	1	2	3	4	5	6
1991-2010	0.420407	0.681923	0.559854	0.990239	0.696034	0.808617	0.625549
1992-2011	0.441583	0.721366	0.579787	1.006666	0.724914	0.826765	0.646448
1993-2012	0.473947	0.773227	0.610988	1.042548	0.770370	0.857946	0.683297
1994-2013	0.528367	0.810408	0.650120	1.080593	0.807845	0.889507	0.721842
1995-2014	0.576238	0.834748	0.697879	1.116436	0.838915	0.910153	0.757813
1996-2015	0.590215	0.867254	0.765643	1.146458	0.865153	0.925586	0.785264
1997-2016	0.607134	0.917737	0.813881	1.180373	0.885877	0.945359	0.816865
1998-2017	0.633826	0.942636	0.832498	1.216115	0.927343	0.960772	0.830383
1999-2018	0.651828	0.959198	0.843917	1.238400	0.970619	0.960479	0.847786
2000-2019	0.675728	0.991259	0.890801	1.259634	0.996480	0.956632	0.862788
2001-2020	0.711533	1.020891	0.919701	1.280825	1.026111	0.962611	0.880883
2002-2021	0.742032	1.036525	0.931712	1.294694	1.056997	0.965877	0.890215
2003-2022	0.775667	1.045098	0.952902	1.321351	1.079954	0.974753	0.905321
2004-2023	0.796867	1.052701	0.985476	1.371402	1.117991	0.984458	0.926620
2005-2024	0.793126	1.071300	1.026638	1.410740	1.154461	0.991544	0.953048
2006-2025	0.805018	1.094451	1.065712	1.446901	1.184837	1.005349	0.969315
2007-2026	0.829458	1.102751	1.089889	1.482153	1.204426	1.030607	0.980268
2008-2027	0.851369	1.124305	1.116933	1.517999	1.233243	1.047958	1.001052
2009-2028	0.878194	1.165945	1.141099	1.561671	1.256323	1.067268	1.006868
2010-2029	0.907850	1.193680	1.174338	1.604863	1.274413	1.094007	1.007159
2011-2030	0.920608	1.197095	1.208536	1.647793	1.311962	1.114079	1.009983
2012-2031	0.938091	1.203983	1.256200	1.689770	1.349701	1.134575	1.028743
2013-2032	0.972313	1.229781	1.297763	1.711150	1.363646	1.151188	1.041233
2014-2033	0.985339	1.264282	1.326705	1.746743	1.393176	1.162837	1.044680
2015-2034	0.992159	1.291048	1.357726	1.782475	1.436793	1.187407	1.051620
2016-2035	1.019948	1.313105	1.388891	1.820207	1.469664	1.216574	1.067582

Table 2.2 Number of ensemble members for each GMST change, including those higher than 4.5°C (which are not used subsequently).

GMST change (°C from pre-industrial)	# ensemble members (RCP8.5)	% of missing ensemble members
1.0	3000	0.0
1.5	3000	0.0
2.0	3000	0.0
2.5	2997	0.1
3.0	2919	2.7
3.5	2700	10.0
4.0	2213	26.2
4.5	1578	47.4
5.0	989	67.0
5.5	515	82.8
6.0	213	92.9

Box 1: Calculating time-slice mean changes from time-series of anomalies using alternative baselines; absolute anomalies

For each UKCP18 probabilistic projection sample, there are time-series of anomalies from the Baseline time-slice B (1981-2000), for the required baseline time-slice R (e.g. 1961-1990) and the required future time-slice F (e.g. 2070-2099). For absolute anomalies (e.g. for temperature projections), these are given by

$$\widehat{R}_t^B = R_t - \bar{B}$$

$$\widehat{F}_t^B = F_t - \bar{B}$$

where $\widehat{}$ indicates anomalies (with the superscript indicating the baseline period from which they are taken), $\bar{}$ indicates the time-slice mean, and t is each time-step in the time-series.

But the anomalies for the future time-slice are required relative to the baseline R rather than the actual baseline B . So

$$\widehat{F}_t^R = F_t - \bar{R} = F_t - \bar{B} + \bar{B} - \bar{R} = \widehat{F}_t^B + \bar{B} - \bar{R}.$$

Given that

$$\bar{R} = \frac{1}{N} \sum_{t=1}^M R_t = \frac{1}{N} \sum (\widehat{R}_t^B + \bar{B}) = \frac{1}{N} \sum \widehat{R}_t^B + \bar{B} = \overline{\widehat{R}_t^B} + \bar{B},$$

where N is the time-slice length, then

$$\widehat{F}_t^R = \widehat{F}_t^B + \bar{B} - \bar{R} = \widehat{F}_t^B - \overline{\widehat{R}_t^B}.$$

Thus the time-slice mean changes for the future time-slice F relative to the required baseline time-slice R can be calculated as

$$\overline{\widehat{F}_t^R} = \frac{1}{N} \sum (\widehat{F}_t^B - \overline{\widehat{R}_t^B}) = \overline{\widehat{F}_t^B} - \overline{\widehat{R}_t^B}.$$

That is, the difference between the time-slice mean change for the future time-slice F relative to the baseline time-slice B , and the time-slice mean change for the required baseline time-slice R relative to the baseline time-slice B .

2.3 Precipitation changes

Sets of precipitation changes are required for each GMST change, for each selected ensemble member/time-slice combination (Section 2.2). These are calculated from the UKCP18 probabilistic projections for river-basin regions (Met Office Hadley Centre 2018), which provides precipitation anomalies for each month and year (Dec 1960-Nov 2099), as percentage differences relative to a baseline of 1981-2000.

For each GMST change and ensemble member, the mean monthly precipitation changes for the required 20-year future time-slice are calculated (using a 1961-1990 baseline) from the year-by-year anomalies (1981-2000 baseline) [see Box 2, page 10]. Note that the Met Office clip (winsorize) extreme precipitation change values, and recommend doing so in the calculation of time-slice means, so values below the 1st percentile (above the 99th percentile) are reset to the 1st percentile (99th percentile) (Met Office 2019).

A single-harmonic function is then fitted to each set of monthly precipitation changes;

$$X(t) = X_0 + A \cos [2\pi (t - \Phi) / 12]$$

with $X(t)$ change for month t , harmonic mean X_0 (mean annual change), harmonic amplitude A (height of peak above mean) and harmonic phase Φ (month of peak). The parameters X_0 and A are the ones used for the axes of the flood response surfaces (Section 2.1). Figure 2.6 shows contour plots of the precipitation projections (as X_0 vs A) for each required GMST change. These show that the projections typically get more seasonal (higher A) as the GMST change increases. The mean annual precipitation change (X_0) can remain similar or can slightly decrease or increase, depending on the region, as the GMST change increases.

To test whether the incomplete ensembles for higher GMST changes are likely to lead to skewed flood peak changes, the precipitation changes for some of the lower GMST changes (with full ensembles) are split into three subsets by the time in the future at which the required GMST is reached. Contour plots comparing the subsets show that ensemble members where the GMST change is reached later in the century tend to have some differences in the distribution of their corresponding precipitation changes, particularly in terms of greater seasonality (higher A), than those that reach the GMST change earlier. Examples plots for the 2.0°C GMST change are shown in Figure 2.7.

The dependence between the precipitation changes and the time in the future at which a certain GMST change is reached means that there will be bias in the flood peak changes extracted for incomplete ensembles (GMST changes of 3.0°C and above) as opposed to complete ensembles (GMST changes of less than 3.0°C). Thus a bias correction technique has been developed to account for this bias (Section 2.6).

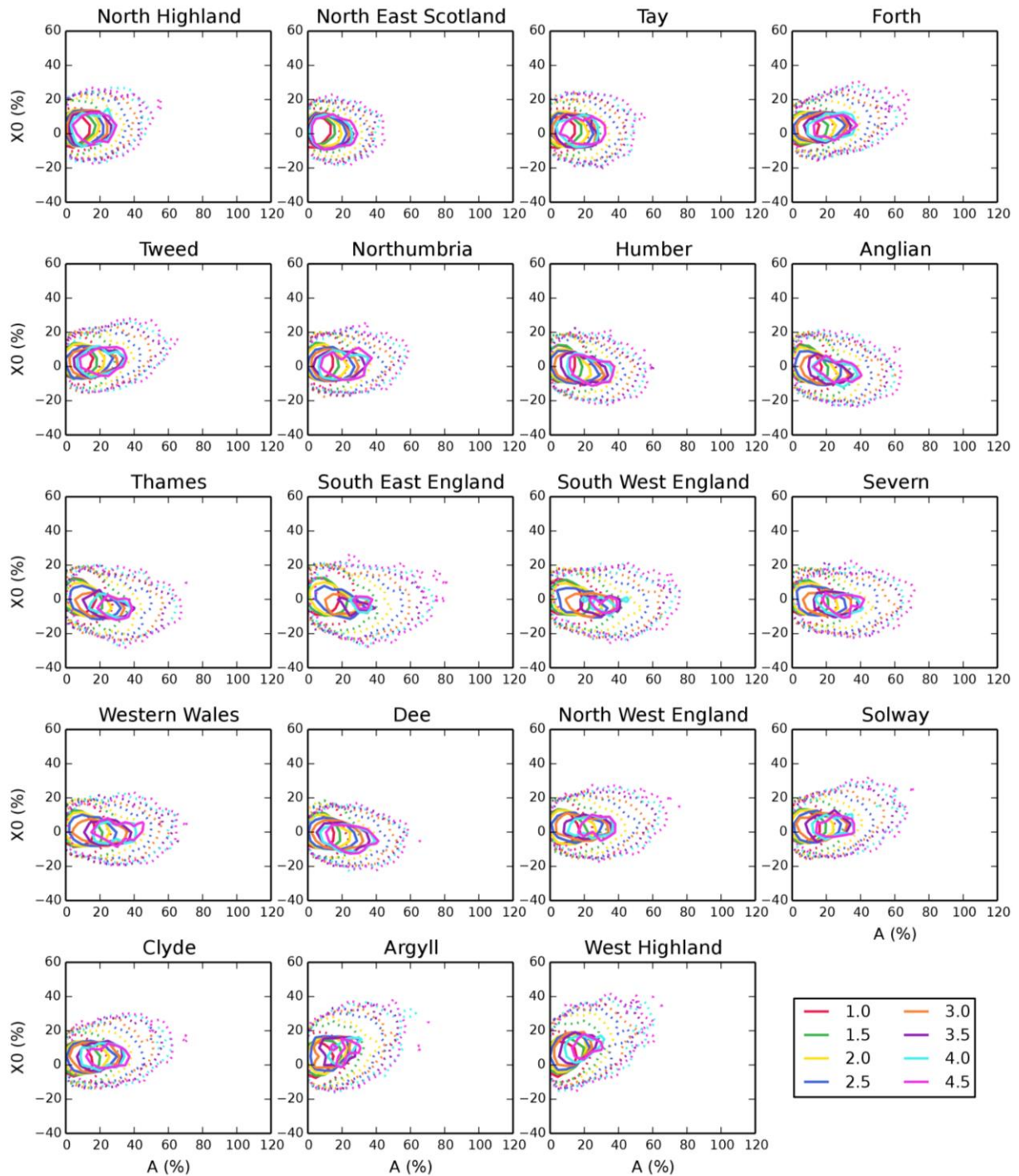


Figure 2.6 Contour plots showing the UKCP18 precipitation harmonic mean (X_0) versus amplitude (A) for each river-basin region, for each required GMST change (RCP8.5). Contours delineate densities of 0.25% and 2.5% of projections per 5% \times 5% sensitivity domain square (dotted and solid lines).

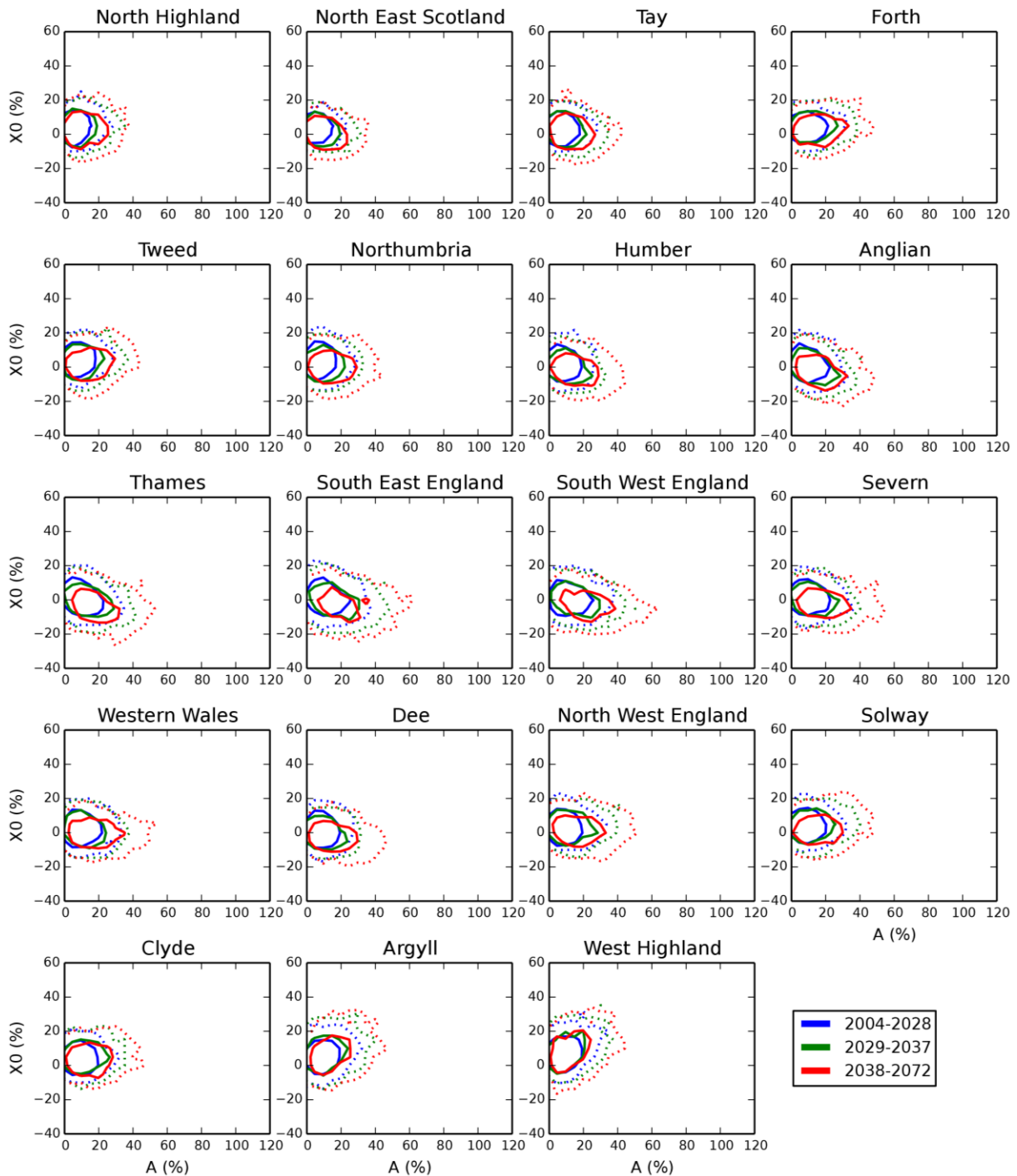


Figure 2.7 Contour plots showing the UKCP18 precipitation harmonic mean (X_0) versus amplitude (A) for each river-basin region, for a 2.0°C GMST change (RCP8.5). The 3000-member ensemble is split into three subsets by the start year of the 20-year time-slice when the GMST change is reached, with roughly 1/3 of the ensemble members in each subset (see key). Contours delineate densities of 0.25% and 2.5% of projections per 5% \times 5% sensitivity domain square (dotted and solid lines respectively).

Box 2: Calculating time-slice mean changes from time-series of anomalies using alternative baselines; percentage anomalies

For each UKCP18 probabilistic projection sample, there are time-series of anomalies from the Baseline time-slice B (1981-2000), for the required baseline time-slice R (e.g. 1961-1990) and the required future time-slice F (e.g. 2070-2099). For percentage anomalies (e.g. for precipitation projections), these are given by

$$\widehat{R}_t^B = (R_t - \bar{B})/\bar{B} * 100 = ((R_t/\bar{B} - 1) * 100$$

$$\widehat{F}_t^B = (F_t - \bar{B})/\bar{B} * 100 = ((F_t/\bar{B} - 1) * 100$$

where \wedge indicates anomalies (with the superscript indicating the baseline period from which they are taken), $\bar{}$ indicates the time-slice mean, and t is each time-step in the time-series.

But the anomalies for the future time-slice are required relative to the baseline R rather than the actual baseline B . So

$$\widehat{F}_t^R = \left(\frac{F_t}{\bar{R}} - 1 \right) * 100 = \left(\frac{\bar{B}}{\bar{R}} \left(\frac{\widehat{F}_t^B}{100} + 1 \right) - 1 \right) * 100 .$$

Given that

$$\bar{R} = \frac{1}{N} \sum_{t=1}^N R_t = \frac{\bar{B}}{N} \sum (\widehat{R}_t^B / 100 + 1),$$

where N is the time-slice length, then

$$\frac{\bar{R}}{\bar{B}} = \frac{1}{N} \sum \left(\frac{\widehat{R}_t^B}{100} + 1 \right) = \frac{1}{N} \left(\sum \frac{\widehat{R}_t^B}{100} + N \right) = \frac{\overline{\widehat{R}_t^B}}{100} + 1,$$

and so

$$\widehat{F}_t^R = (\widehat{F}_t^B - \overline{\widehat{R}_t^B}) / \left(\frac{\overline{\widehat{R}_t^B}}{100} + 1 \right).$$

Thus the time-slice mean changes for the future time-slice F relative to the required baseline time-slice R can be calculated as

$$\overline{\widehat{F}_t^R} = \frac{1}{N} \sum \left(\widehat{F}_t^B - \overline{\widehat{R}_t^B} \right) / \left(\frac{\overline{\widehat{R}_t^B}}{100} + 1 \right) = \left(\overline{\widehat{F}_t^B} - \overline{\widehat{R}_t^B} \right) / \left(\frac{\overline{\widehat{R}_t^B}}{100} + 1 \right).$$

That is, the difference between the time-slice mean change for the future time-slice F relative to the baseline time-slice B , and the time-slice mean change for the required baseline time-slice R relative to the baseline time-slice B , with an additional divisor that allows for the use of percentage rather than absolute anomalies (cf Box 1, page 6).

2.4 Flood peak changes for Great Britain

For each selected time-slice/RCP combination, the precipitation changes were overlaid (as X_0 vs A) on the flood response surfaces derived in the EA project (Section 2.1), for each 1km river cell. Specifically, the response surfaces for changes in 50-year return period flood peaks (for the Medium–August temperature/potential evaporation scenario) were applied, with the extra uncertainty allowances (Kay et al. 2020). This approach is illustrated in Figure 2.8.

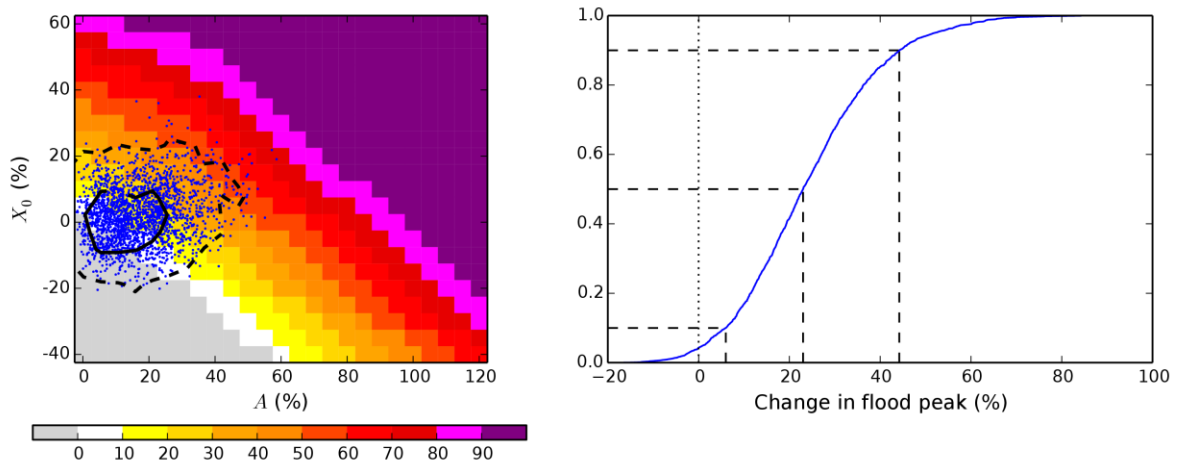


Figure 2.8 Schematic showing the method for estimating flood peak changes from UKCP18 precipitation changes, for a single 1km river cell. The UKCP18 climate change projections corresponding to a given GMST change are overlaid on a modelled response surface (left). Blue dots show each of the 3,000 projections for the appropriate river-basin region. Black contours delineate densities of 0.25% and 2.5% of projections (dashed and solid lines) per 5% \times 5% sensitivity domain square. Also shown is the cdf of the percentage changes in flood peaks extracted from the response surface (including the appropriate extra uncertainty allowance) with the 10th, 50th and 90th percentiles indicated by dashed lines (right). This illustration is for a location in north-west Scotland (Easting 268500 Northing 961500, in the North Highlands river-basin region), under a 4°C GMST change using RCP8.5 emissions. The method is repeated for each 1km river cell in GB (12,421 points), and for each required GMST change/RCP combination.

Grids of 50th percentile changes in 50-year return period flood peaks were produced for each GMST change/RCP combination. As an example, Figure 2.9 maps the 50th percentile of change in 50-year return period flood peaks under a 2.5°C GMST change using RCP8.5 emissions. This shows significant spatial variation, with impacts typically higher in the west than the east. For GMST changes above 2.5°C, bias correction grids need to be added to the grids of 50th percentile flood peak changes (Section 2.6). Additional grids of 10th and 90th percentiles changes were produced for those GMST changes with (essentially) full 3000-member ensembles (1.0, 1.5, 2.0 and 2.5°C; Table 2.2), to allow an assessment of climate modelling uncertainty.

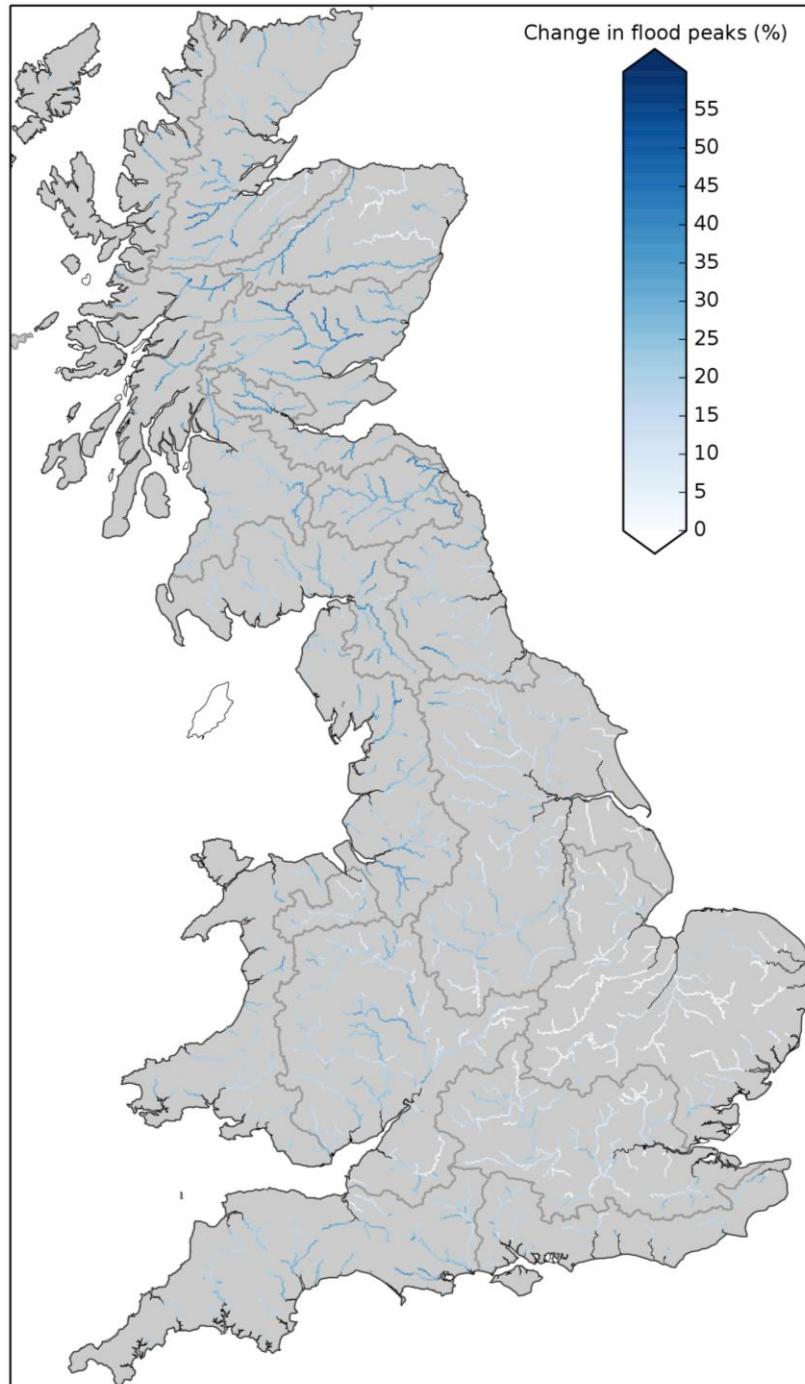


Figure 2.9 Map showing the 50th percentile of change in 50-year return period flood peaks under a 2.5°C GMST change using RCP8.5 emissions.

To enable easier comparison of flood peak changes, results are summarized as the regional mean and standard deviation (SD), for each of the 19 GB river-basin regions (Figure 2.2). Maps of regional means for the 50th percentile change in 50-year return period flood peaks, for the four lower GMST changes (1.0-2.5°C) under RCP8.5 emissions (Figure 2.10 middle), show increases in flood peaks with some variation between regions. In contrast, the 10th percentile changes (Figure 2.10 left) show decreases in flood peaks in some regions. The 90th percentile changes (Figure 2.10 right) can be significantly higher than the 50th percentile changes, especially for higher GMST changes.

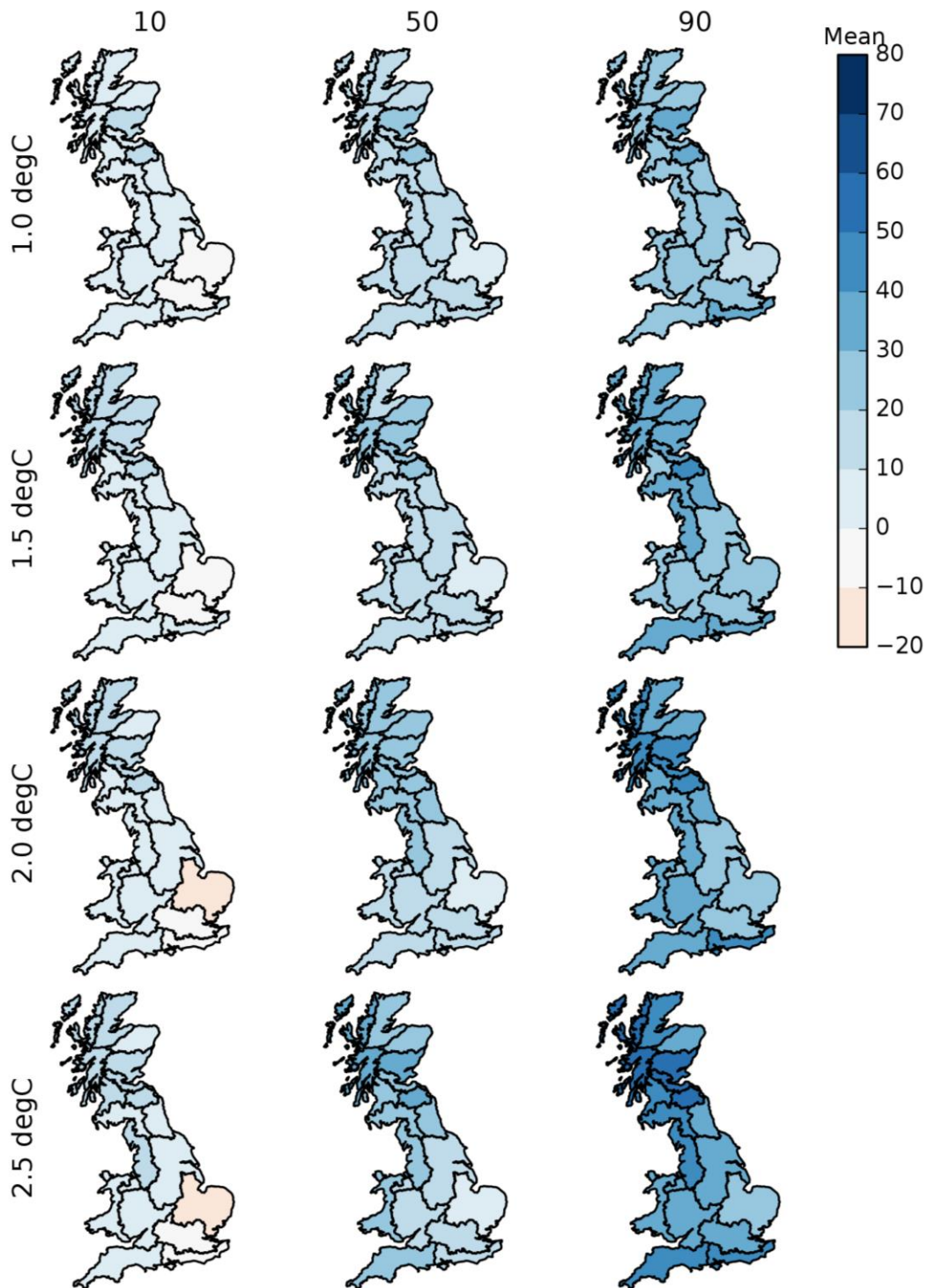


Figure 2.10 Maps showing the regional means of the 10th, 50th and 90th percentile changes in 50-year return period flood peaks for four GMST changes under RCP8.5 emissions.

Maps of regional SDs (Figure 2.11) generally show higher SD for higher percentiles and higher GMST changes, but some regions have consistently higher SD (i.e. intra-regional variation in impacts) than others.

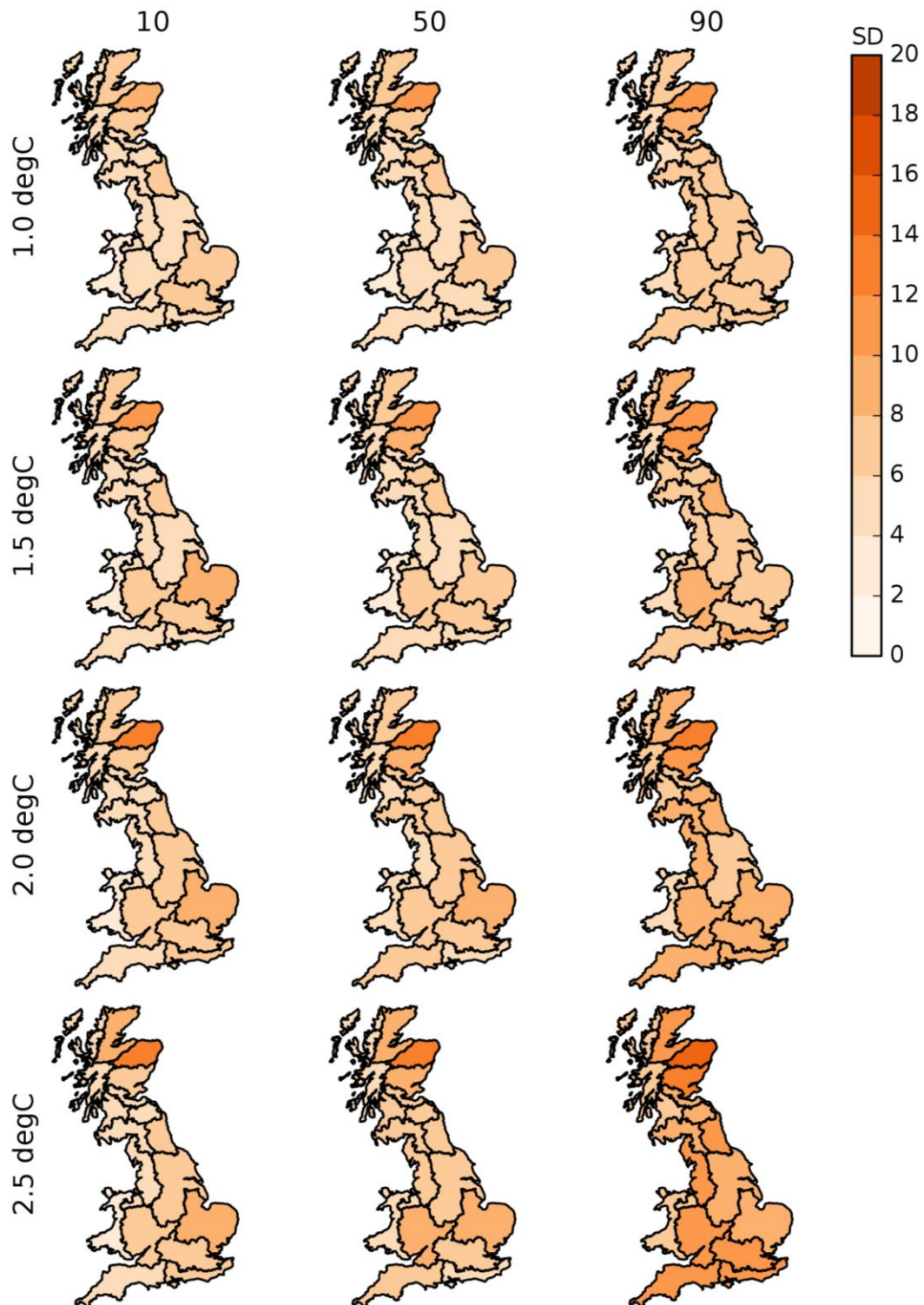


Figure 2.11 Maps showing the regional standard deviations of the 10th, 50th and 90th percentile changes in 50-year return period flood peaks for four GMST changes under RCP8.5 emissions.

2.5 Flood peak changes for Northern Ireland

The national-scale sensitivity framework modelling described in Section 2.1 does not provide any information for Northern Ireland (NI), and to our knowledge there is no equivalent work that does, so for NI a simpler approach was taken, but one still based on the sensitivity framework. For each of the three river-basin regions covering

NI (Figure 2.12a), the precipitation changes derived from the UKCP18 probabilistic projections (Figure 2.12b) were overlaid on the representative flood response surface for the 'Neutral' response type. The Neutral response type is the one most prevalent in the north/west of GB (Kay et al. 2014a), so represents the best guess of the response type for catchments in Northern Ireland. This was done for each required time-slice/RCP combination, and the percentiles provided as for GB. For GMST changes above 2.5°C, bias correction values still need to be added to the 50th percentile flood peak changes (Section 2.6).

a)



b)

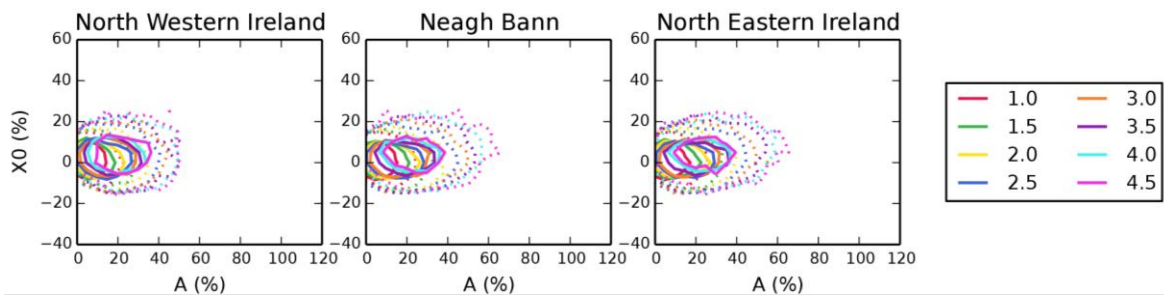


Figure 2.12 a) The three river-basin regions covering NI. b) Contour plots showing UKCP18 precipitation harmonic mean (X_0) versus amplitude (A) for each river-basin region, for each required GMST change (RCP8.5). Contours delineate densities of 1.8% of projections per 5% \times 5% sensitivity domain square.

Maps of the regional changes in 50-year return period flood peaks, for the four lower GMST changes (1.0-2.5°C) under RCP8.5 emissions (Figure 2.13), show increases in flood peaks for all percentiles, all GMST changes, and all regions, with limited variation between regions.

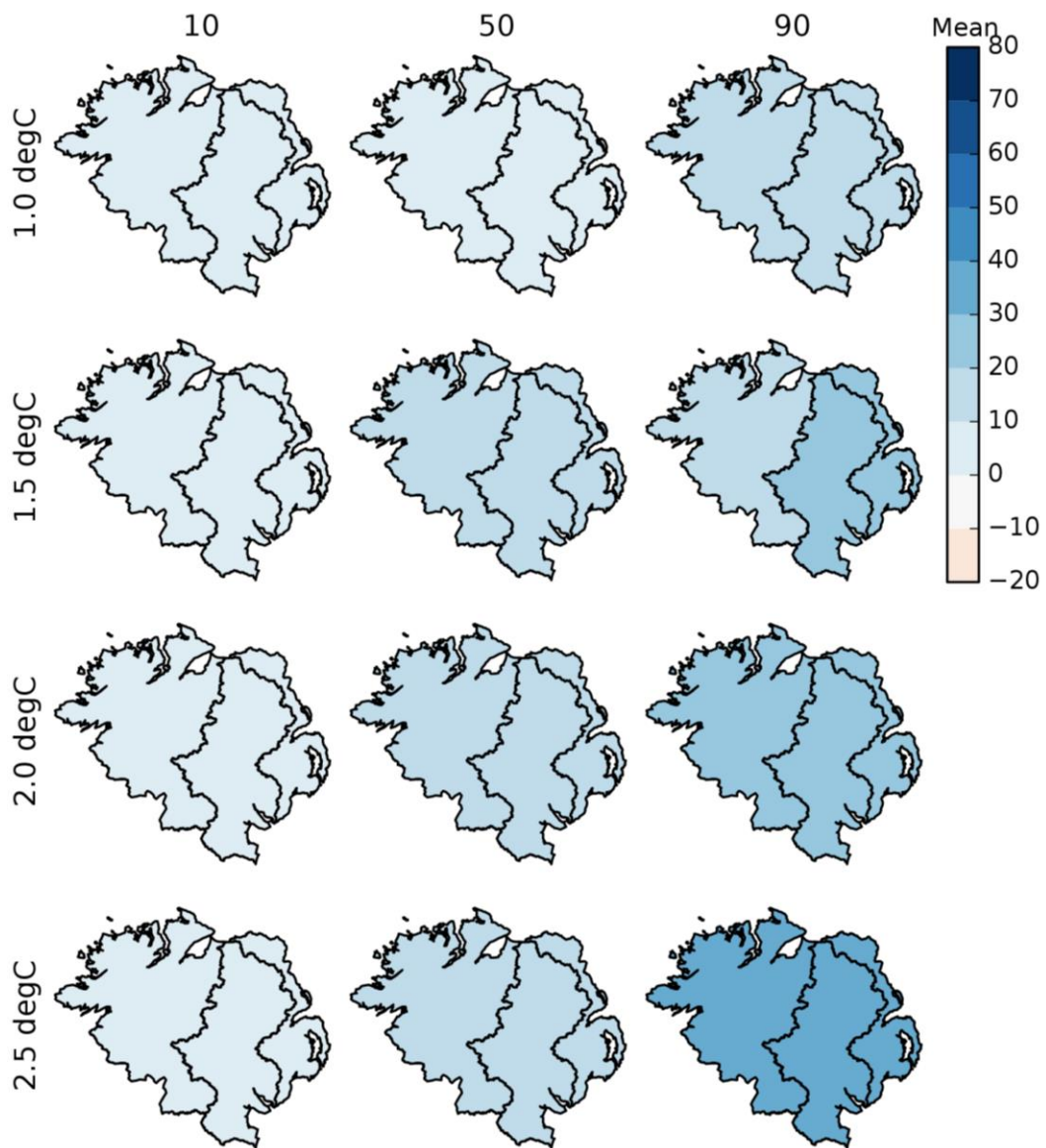


Figure 2.13 Maps showing the 10th, 50th and 90th percentile changes in 50-year return period flood peaks for the three river-basin regions covering NI, for four GMST changes under RCP8.5 emissions.

2.6 Correction of bias in impacts derived from incomplete ensembles

As noted previously, not all required GMST changes have a full set of 3,000 samples (Table 2.2), and dependence between the precipitation changes and the time in the future at which a certain GMST change is reached (Section 2.3) means that there will be bias in the flood peak changes extracted for incomplete ensembles. Thus a bias correction technique has been developed to account for this bias.

To investigate the bias, the percentage of the ensemble members applied is systematically reduced (for GMST changes with full ensembles; 1.5, 2.0 and 2.5°C), to see how much bias this gives in the 50th percentile flood peak change compared to use of the whole ensemble. The percentage reductions in ensemble size applied are those corresponding to each of the required higher GMST changes (3.0, 3.5, 4.0, 4.5°C; Table 2.2), and ensemble members are preferentially removed according to

their corresponding time-slice and precipitation harmonic amplitude A (i.e. they are ordered first by time-slice, earlier to later, then by A , low to high, and ensemble members are systematically removed from the end of the ordered list). The biases derived for each percentage reduction in ensemble size for the lower GMST changes are then extrapolated, to estimate the biases for each of the required higher GMST changes. The ensemble corresponding to a 1.0°C GMST change is not used as part of the extrapolation, despite being a complete ensemble, as its strong concentration to the left-hand side of the sensitivity domain (Figure 2.6), regardless of time-slice, when combined with the response surfaces, introduces ‘noise’ into the extrapolation.

The sets of projections for each river-basin region are overlaid on the representative flood response surface for each of the nine response types (Section 2.1), rather than on the 1km modelled response surfaces, to make the extrapolation fitting feasible; one line for each river-basin region, response type, and percentage reduction in ensemble size. Figure 2.14 shows an example of the biases derived for two combinations of river-basin region and response type, for the four percentage reductions in the ensemble size (2.7, 10.0, 26.2 and 47.4%; Table 2.2). It also shows the extrapolation of the biases for each of the corresponding higher GMST changes (3.0, 3.5, 4.0 and 4.5°C), which is done as follows;

- Fit a straight line through the points for 1.5, 2.0 and 2.5°C.
- If the slope of the line is ≤ 0 , extrapolate the line to the required GMST change (e.g. Figure 2.14a).
- If the slope of the line is > 0 (i.e. it would result in smaller estimates of bias, and possibly positive biases, for higher GMST changes), calculate the mean value of the points and use that to extrapolate instead (e.g. red and green lines/dots in Figure 2.14b).

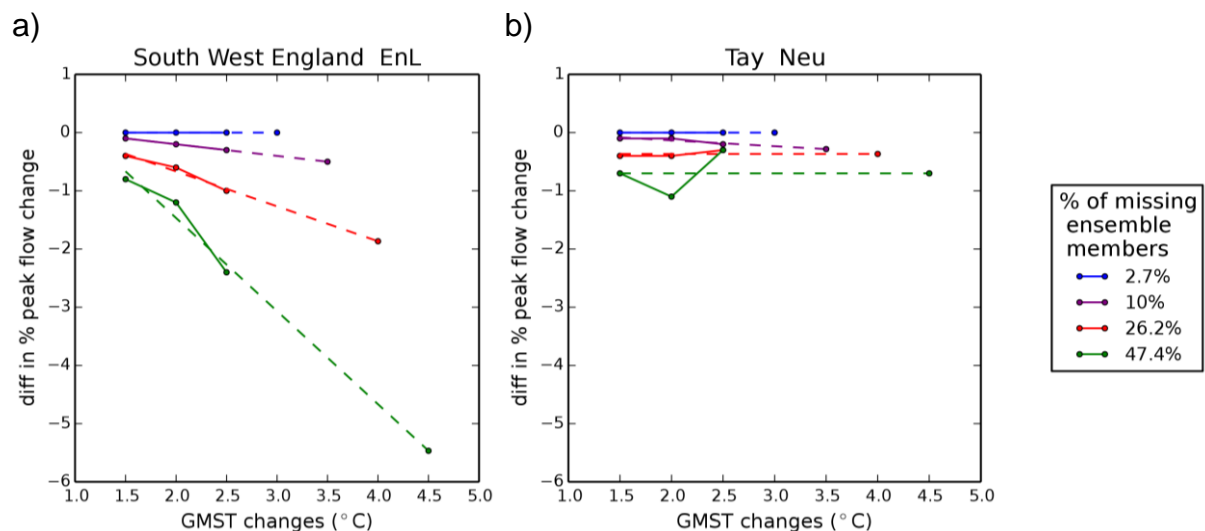


Figure 2.14 Example extrapolation of the bias in 50th percentile flood peak change between the full and reduced ensembles for higher GMST changes: a) Enhanced-Low response type in the South West England region, b) Neutral response type in the Tay region.

Table 2.3 Estimated biases for two river-basin regions in GB, for each response type and each of the required higher GMST changes.

Response type	South West England				Tay			
	3.0°C	3.5°C	4.0°C	4.5°C	3.0°C	3.5°C	4.0°C	4.5°C
DpE	0.0	-0.1	-0.8	-1.5	0.0	0.1	0.0	0.5
DpH	0.0	-0.3	-1.1	-1.5	0.0	-0.1	-0.2	0.2
DpL	0.0	-0.2	-1.3	-3.5	0.0	-0.4	-0.4	-0.3
Neu	0.0	-0.3	-1.7	-4.4	0.0	-0.3	-0.4	-0.7
Mix	0.0	-0.3	-1.2	-2.4	0.0	-0.2	-0.4	-0.2
EnL	0.0	-0.5	-1.9	-5.5	0.0	-0.1	-0.4	-0.7
EnM	0.0	-0.4	-1.9	-5.1	0.0	-0.3	-0.2	-0.5
EnH	0.0	-1.0	-3.1	-6.7	0.0	-0.5	-0.4	-0.7
Sen	0.0	-0.5	-2.4	-4.7	0.0	-0.4	-0.2	-0.2

This process results in a table of estimated biases for each GB river-basin region, response type and required higher GMST change (3°C and above). The biases vary substantially by region and response type and generally increase with GMST change (Table 2.3), as would be expected with the increase in the percentage of the ensemble missing for higher GMST changes. The bias table was then used to assign a bias correction value (set to minus the bias) to each 1km river cell (catchment area $\geq 100\text{km}^2$). Any bias corrections below zero are set to zero, to avoid reducing the percentage change in flood peak. Figure 2.15 shows the bias correction grids for each GMST change with an incomplete ensemble (3°C and above). The GB bias correction grids are provided alongside the 50th percentile flood peak change grids, and the corresponding pairs should be added together.

To illustrate the difference that the bias corrections make to the sequence of changes in flood peaks as GMST change increases, Figure 2.16 shows the regional means of the 50th percentile flood peak changes both with and without the grids of bias corrections applied. This shows that the bias corrections make a relatively significant difference in some regions, especially for a 4.5°C GMST change. Also shown in Figure 2.16 are the regional means of the 10th and 90th percentile flood peak changes for the lower GMST changes, to illustrate the wide range of uncertainty from the UKCP18 probabilistic projections. In addition, Figure 2.17 shows the regional standard deviations of the 50th percentile flood peak changes both with and without the grids of bias corrections applied, illustrating that intra-regional differences in the bias corrections affect the intra-regional variation in flood peak changes.

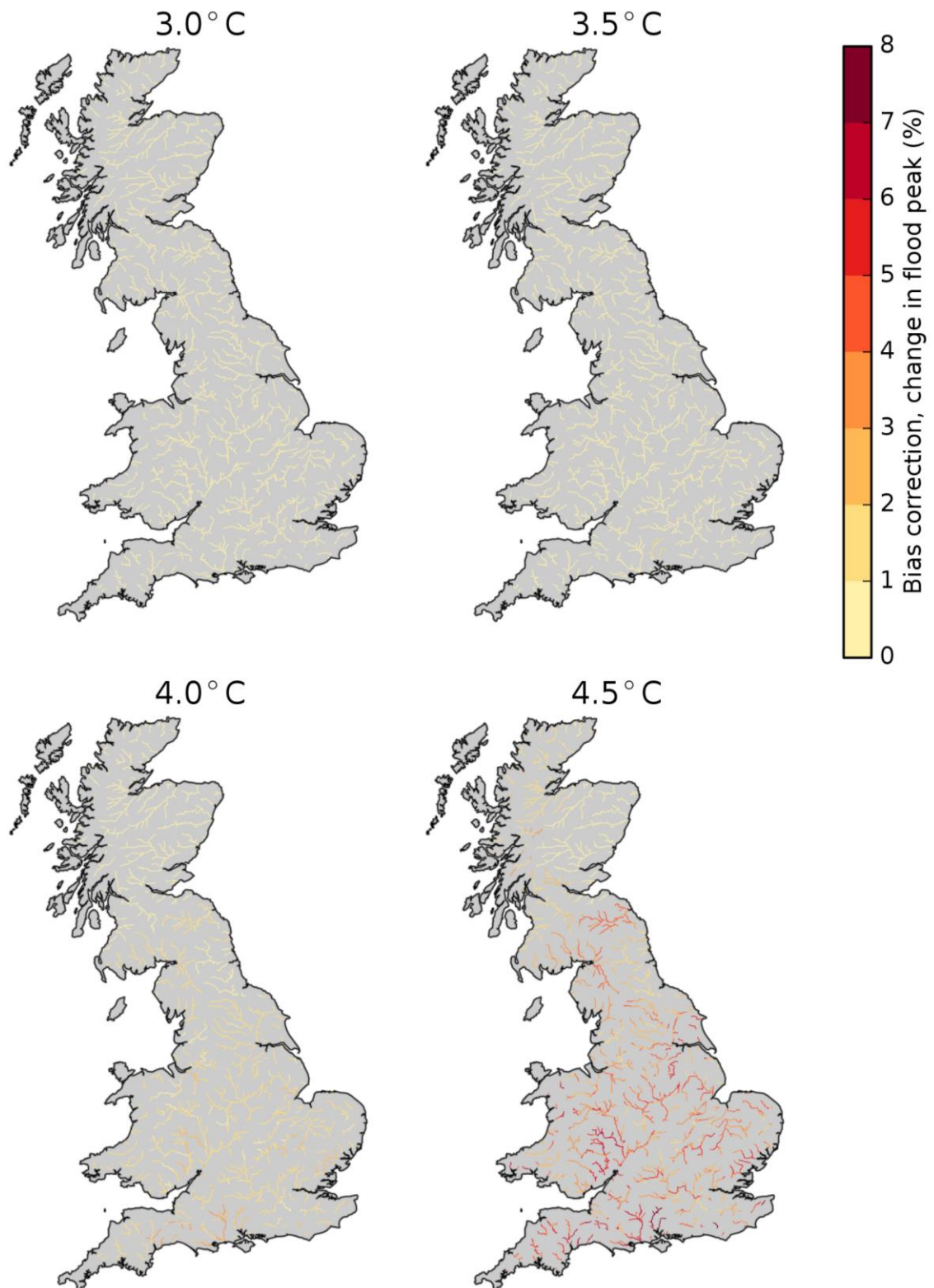


Figure 2.15 Bias correction grids for 50th percentile changes in 50-year return period flood peaks, for each GMST change with an incomplete ensemble.

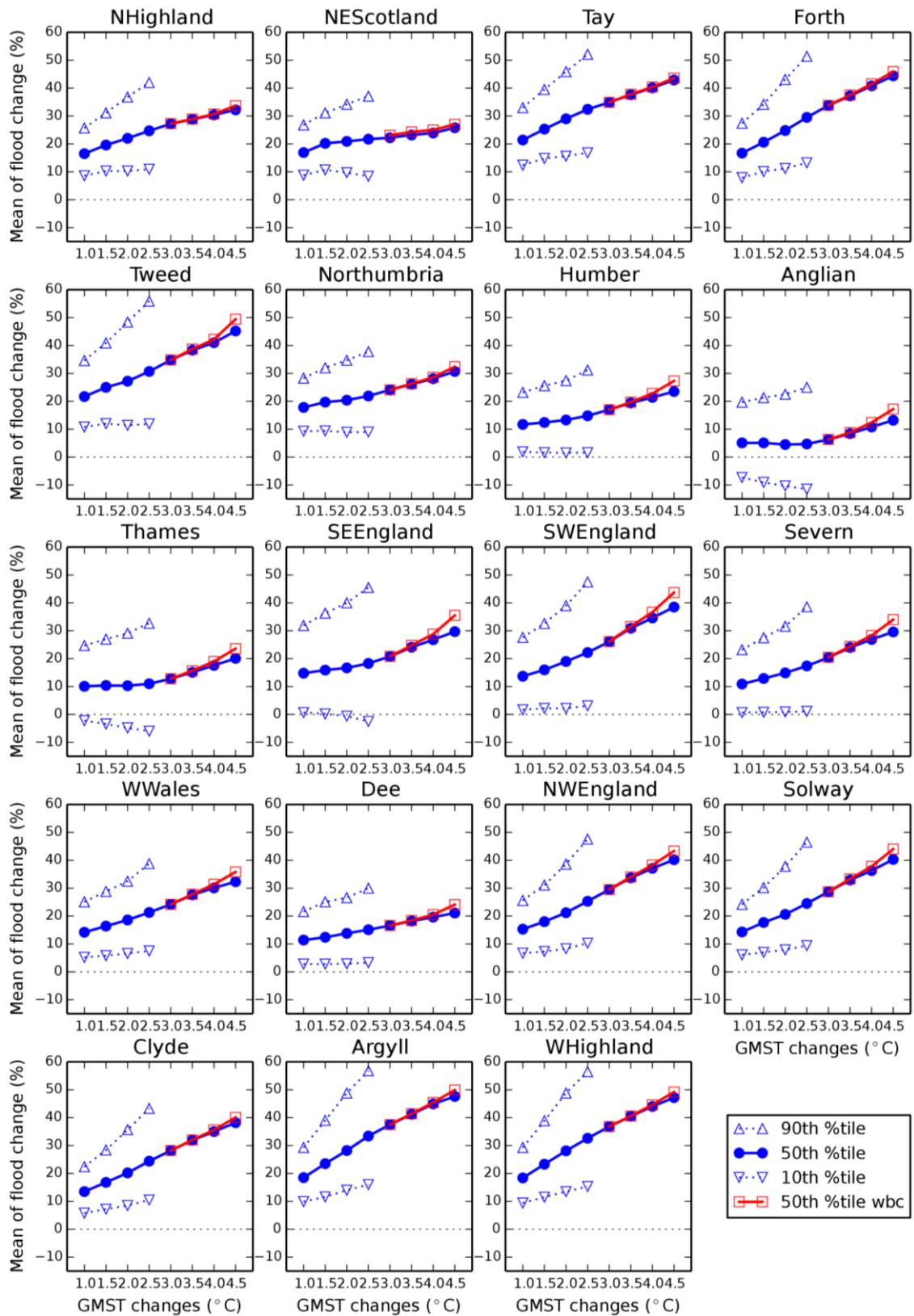


Figure 2.16 Plots comparing the regional means of changes in 50-year return period flood peaks for the range of GMST changes under RCP8.5 emissions. Each plot shows three percentiles of change (10th, 50th and 90th) for results without bias correction, and the 50th percentile changes with bias correction.

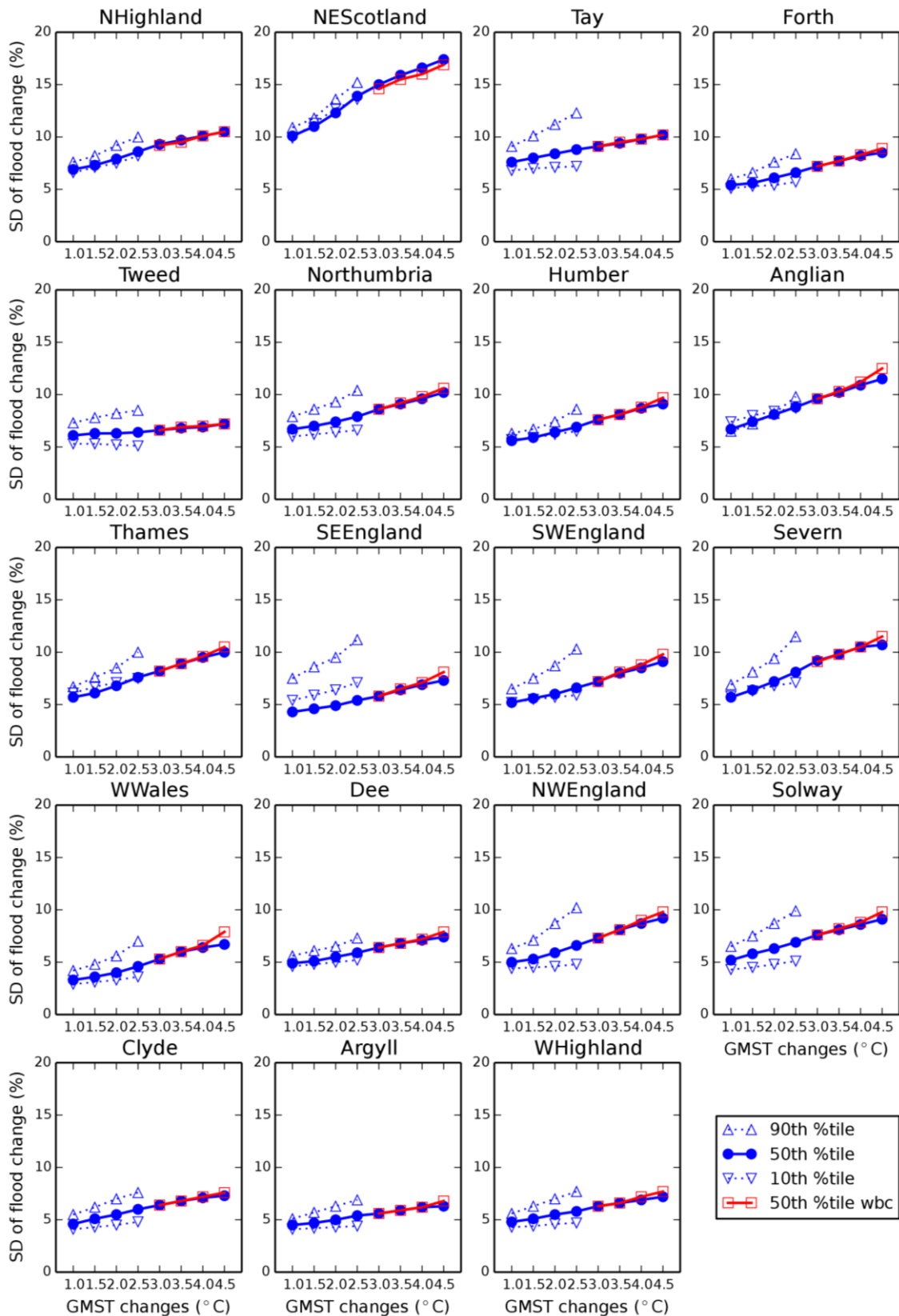


Figure 2.17 Plots comparing the regional standard deviations of changes in 50-year return period flood peaks for the range of GMST changes under RCP8.5 emissions. Each plot shows three percentiles of change (10th, 50th and 90th) for results without bias correction, and the 50th percentile changes with bias correction.

Table 2.4 Estimated biases for the three river-basin regions in NI, for the Neutral response type, for each of the required higher GMST changes.

Region	3.0°C	3.5°C	4.0°C	4.5°C
North Western Ireland	0.0	-0.3	-1.3	-2.7
Neagh Bann	0.0	-0.4	-1.4	-2.6
North Eastern Ireland	0.0	-0.4	-1.3	-2.3

Biases are also estimated for the three river-basin regions in NI for each required higher GMST changes (Table 2.4), but only using the Neutral response type as applied for estimating the flood peak changes in NI (Section 2.5). The bias corrections are set to minus the respective biases.

2.7 Uncertainty from emissions trajectory

Another source of uncertainty could be the RCP trajectory, as a given GMST change can be obtained from simulations with different RCP trajectories. Figure 2.18 shows the difference between the 50th percentile change in flood peaks for three different RCP trajectories (RCP2.6, RCP4.5, RCP6.0) when compared to flood peak changes from RCP8.5, for a GMST change of 1.5°C. The differences are summarised by the minimum, median and maximum for 1km river points in each GB region. Figure 2.19 shows the equivalent differences for the three regions of NI (although the data for NI are not spatial). The RCP trajectory used makes a difference to the impact estimates for a given GMST change, however use of RCP8.5 emissions always gives the largest impacts of the four RCPs, and the differences are relatively small for the 50th percentile change. For GB, the estimates differ from the RCP8.5 value by 0.5-4.7% for RCP2.6, 0.1-2.9% for RCP4.5 and 0.1-3.4% for RCP6.0.

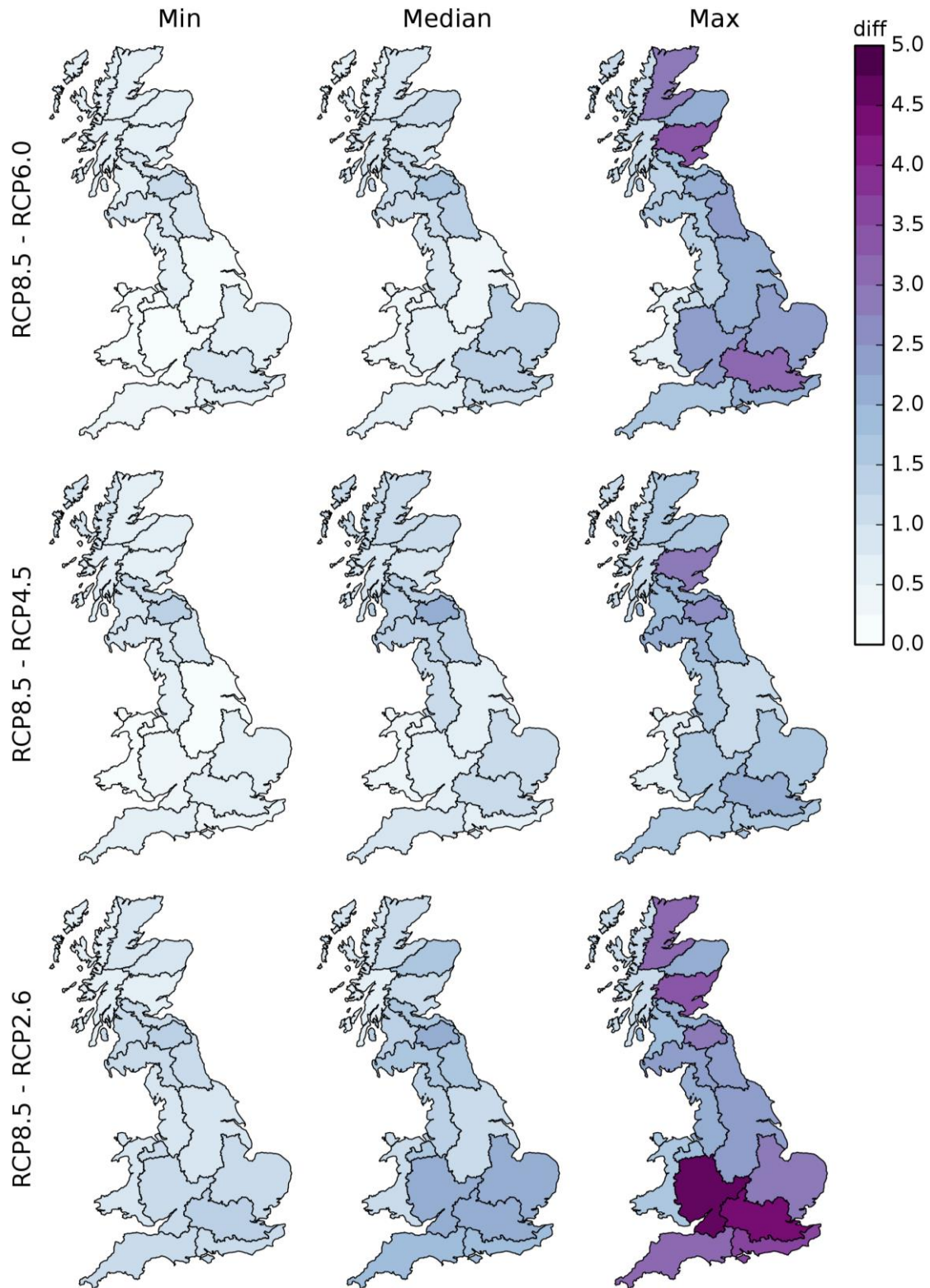


Figure 2.18 Maps showing the regional minimum, median, maximum of the difference between the 50th percentile changes in flood peaks for RCP8.5 compared to RCP6.0, RCP4.5 and RCP2.6, for a GMST change of 1.5°C.

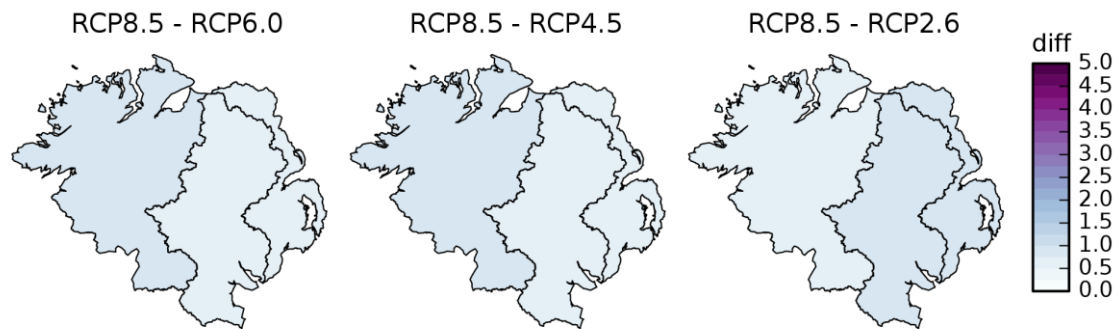


Figure 2.19 Maps showing the regional difference between the 50th percentile changes in flood peaks for RCP8.5 compared to RCP6.0, RCP4.5 and RCP2.6, for a GMST change of 1.5°C, for the three river-basin regions covering NI.

2.8 Additional information

The response surfaces derived for the EA project (Section 2.1) can only provide information on flood peak changes for 1km cells in GB with a catchment area $\geq 100\text{km}^2$ (1km river cells). To enable estimation of changes in flood peaks for 1km cells in GB with smaller catchment areas, a look-up table was provided which gives (where possible) the coordinates of the nearest downstream 1km river cell (area $\geq 100\text{km}^2$). Any 1km cells that flow into the sea without reaching a 1km river cell are not included in the look-up table.

3 Changes in return periods

To assess the impact of climate change on flooding, changes in flood peaks need to be translated to changes in return period. In the CCRA2 this was done using regional growth curves taken from the Flood Studies Report (NERC, 1975). For the current project, the approach has been improved and updated to make use of Flood Estimation Handbook (FEH) methods (Institute of Hydrology, 1999).

3.1 Mapping 1km river cells to 50m pixels

For GB and NI a process of assigning FEH statistics to each 1km river cell was developed. The FEH statistics are available on a 50m resolution grid, therefore the process requires associating an appropriate 50m pixel to each 1km river cell (catchment area $\geq 100\text{km}^2$). Two different methods are used for GB and NI. The approach for GB is more complex as there is a need to ensure that the selected 50m pixels have catchments consistent with those of their corresponding 1km river cells, and thus with the spatial modelling of flood peak changes on a 1km grid for GB (Section 2.4). NI uses a simpler approach as there is no need to ensure spatial consistency (Section 2.5).

In GB, each 1km river cell is assigned a 50m pixel based on matching catchment area. The 50m pixel with the closest catchment area to that of the 1km river cell is assigned to the 1km river cell; this has to be within 10% of the 1km catchment area (Figure 3.1a). If there is not a 50m pixel that has a catchment area within 10% of the 1km catchment area within the 1km river cell, then the 50m pixels within the surrounding eight 1km cells are also assessed (Figure 3.1b). If there is not a 50m

pixel within these surrounding cells that has a catchment area within 10% of the 1km catchment area, no 50m pixel is assigned to the 1km river cell.

A test is used to check that the 50m pixels assigned for each 1km river cell are on the same river network as the 1km river, by tracing upstream of the 1km river cells and selected 50m pixels to check that they flow through the same set of 1km cells. Any 50m pixels that are not on the correct river are removed and the corresponding 1km river cell is not assigned a 50m pixel.

Most 1km river cells (99.98%) have an appropriate 50m pixel within the cell. After inclusion of 50m pixels selected from the surrounding eight 1km cells of a 1km river cell, and after removal of 50m pixels which are located on an incorrect river, 99.99% of 1km river cells have an assigned 50m pixel. This leaves 163 1km river cells without an assigned 50m pixel. Most (58%) of these remaining 1km river cells can be infilled using a downstream 1km river cell, the coordinates of which are provided in the look-up table described in Section 2.8. The small number of 1km river cells that have no associated 50m pixel and that flow into the sea without entering a downstream 1km river cell with an assigned 50m pixel are not included in the look-up table.

For NI, the process of associating a 50m pixel with a 1km cell is simpler than for GB; the 50m pixel with the maximum catchment area within a 1km cell is used to represent the 1km cell. Again only 1km cells with a catchment area $\geq 100\text{km}^2$ are included.

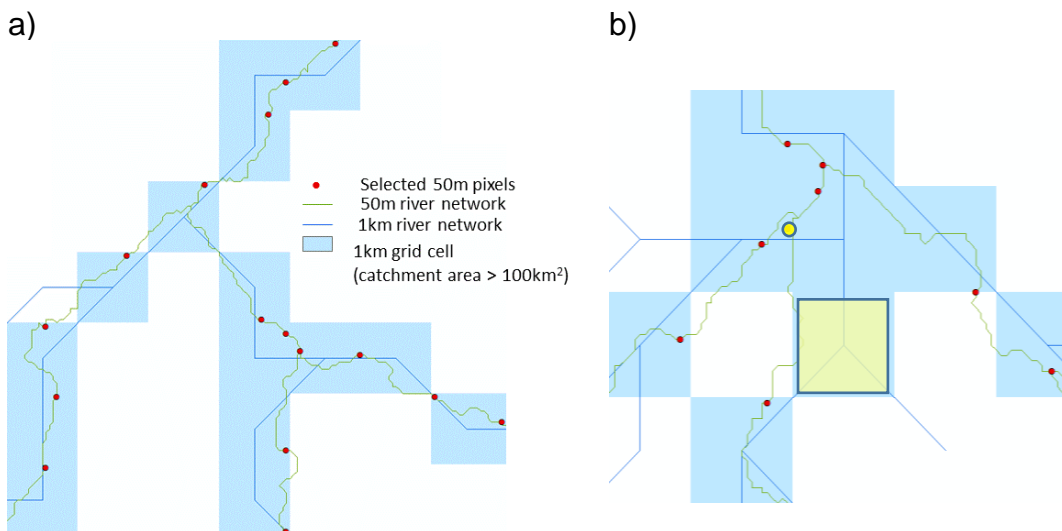


Figure 3.1 a) Example showing 50m pixels (red dots) selected within 1km river cells (blue boxes) based on catchment area. b) Example where a selected 50m pixel (yellow circle) is outside the corresponding 1km river cell (yellow box).

3.2 Return period analysis for 50m pixels

The FEH statistical method (Kjeldsen et al. 2008) is the UK national standard for flood frequency estimation, by which a river flow at any location on the digital river network can be assigned a return period, or average recurrence interval. The method is based on the index flood technique, where the index variable is the median annual flood (*QMED*), and this is combined with a statistical growth curve relating flood peak to return period. For ungauged sites, *QMED* can be estimated via a regression equation based on hydrological catchment descriptors, while the growth curve is

derived from a flexible regionalisation procedure within which annual maximum flow data (*AMAX*) from hydrologically similar sites (pooling-groups) are pooled together.

The FEH statistical method was applied at each of the 1km cells draining an area of at least 100km² in GB and NI where percentage changes in flood peaks had been estimated (Section 3.1), i.e. at 12,282 points in Great Britain and 1,433 points in NI. The first step in the procedure was to extract eight catchment descriptors (Centroid Easting, Centroid Northing, *AREA*, *SAAR*, *FARL*, *BFIHOST*, *URBEXT₂₀₀₀* and *FPEXT*) from Oracle grid tables held at CEH, which allowed *QMED* to be estimated at each 1km grid point. Next, pooled growth curves were derived at each grid point by fitting the Generalised Logistic distribution to pooling-groups formed from the NRFA Peak Flow dataset version 7 (<https://nrfa.ceh.ac.uk/peak-flow-dataset>). The pooled growth curves, when combined with the *QMED* estimates, provided FEH peak flow estimates for a set of return periods ranging from 2 to 1000 years at each grid point.

It should be noted that FEH Vol. 1 (Reed 1999) states that the statistical method is intended principally for use for return periods between 2 and 200 years, and thus the higher return period estimates should be used with caution, especially as the average length of record of the NRFA Peak Flow data is 42 years. However, the FEH statistical method has previously been used for return periods of up to 1000 years in flood mapping studies (EA 2015) and the use of a single estimation procedure across the full range of frequencies was considered to provide consistency.

The FEH flood frequency curve for each grid point was used to estimate the change in the return period of the current *T*-year flood corresponding to a set of percentage changes in flow, as shown schematically in Figure 3.2 and in Table 3.1 for a single point in the dataset.

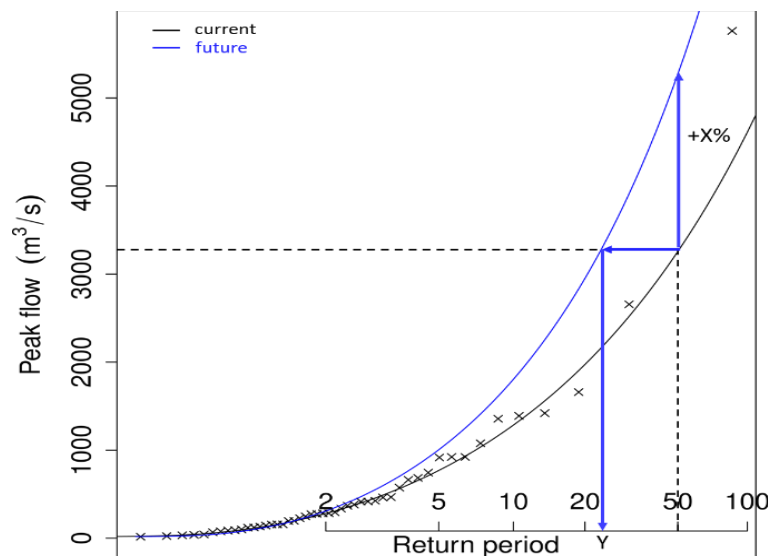


Figure 3.2 Schematic showing method for estimating change in return period from change in peak flow.

Table 3.1 Example relating percentage changes in peak flow to changes in return period. For one point within the dataset (ID 30243, Easting 231500, Northing 717500), a 10% increase in peak flow (+10%) would reduce the return period of a particular flow from 1:100 to 1:59 years.

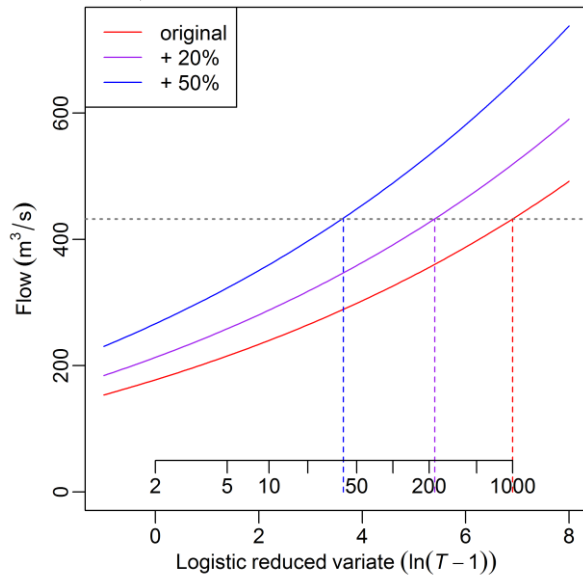
ID: 30243 E: 231500, N: 717500	Current Return Period (years)									
	2	5	10	25	50	75	100	200	500	1000
% change in peak flow	Revised return period (years) given a change in peak flow									
-20%	4.8	16	33	86	173	260	346	690	1717	3419
-10%	2.9	8.4	18	45	90	135	180	359	896	1788
-5%	2.4	6.4	13	33	67	100	133	266	664	1327
+0%	2.0	5.0	10	25	50	75	100	200	500	1000
+5%	1.7	4.0	7.8	19	38	57	76	152	381	764
+10%	1.6	3.3	6.2	15	30	44	59	118	295	590
+15%	1.4	2.8	5.0	12	23	35	46	92	230	461
+20%	1.3	2.4	4.1	9.4	18	27	36	72	182	364
+25%	1.3	2.1	3.4	7.6	15	22	29	58	145	290
+30%	1.2	1.8	2.9	6.3	12	18	23	46	116	233
+40%	1.1	1.5	2.2	4.4	8.1	12	16	31	77	154
+50%	1.1	1.4	1.8	3.3	5.8	8.3	11	21	52	105
+60%	1.1	1.2	1.6	2.6	4.3	6.0	7.8	15	37	73
+80%	1.0	1.1	1.3	1.8	2.6	3.5	4.4	8.0	19	38
+100%	1.0	1.1	1.1	1.4	1.9	2.3	2.8	4.8	11	21
+150%	1.0	1.0	1.0	1.1	1.2	1.3	1.5	2.0	3.7	6.6
+200%	1.0	1.0	1.0	1.0	1.1	1.1	1.2	1.3	1.9	2.9

Figure 3.3 provides examples of two contrasting flood frequency cases, illustrating how the same peak flow change applied in different locations can give very different changes in return period depending on the shape of the baseline flood frequency curve. When a flatter, straighter curve is shifted vertically, there is a large horizontal distance between the curves. When a steep, skewed curve is shifted vertically by the same amount, there is only a small horizontal distance between the curves. The change in horizontal distance relates to the change in return period.

The shape of the baseline curve is governed by the distribution assumed for the annual maximum peak flows and the parameterisation of that distribution. The FEH statistical method assumes the Generalised Logistic as the default distribution for annual maximum peak flows and estimates its parameter values through a pooled frequency analysis. In this method, information is transferred from gauged catchments deemed to be hydrologically similar to the catchment of interest, where similarity is measured through four catchment descriptors: *AREA* (catchment area), *SAAR* (average annual rainfall), *FPEXT* (floodplain extent) and *FARL* (size and location of lakes and reservoirs). The baseline curve is fitted to the gauged annual maxima of all the stations in the pooling-group.

ID: 34478

E: 238500, N: 448500



ID: 172937

E: 685500, N: 218500

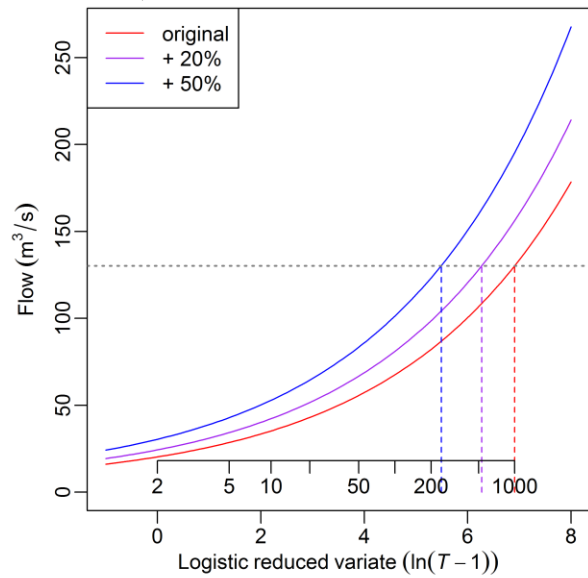


Figure 3.3 Example flood frequency plots for two locations with differently shaped baseline curves, showing how the same flow peak changes (+20% or +50%) can give very different changes in return period, especially for the baseline 1000-year return period flood.

Since two tributaries immediately upstream of a confluence can be very different in terms of area, floodplain extent, and size and location of lakes and reservoirs, it is possible for two nearby locations to have very different flood frequency curves. Further differences in return period may arise from the spatial variability in the percentage change in flood magnitudes on each of the tributaries. Figure 3.4 illustrates this, by plotting the flood frequency curves before and after the change in flood magnitudes for two points upstream and one point downstream of a confluence of the rivers Teme and Corve near Ludlow, Shropshire. The upstream catchments are outlined in purple and green, and the downstream in blue. The river network is coloured according to the percentage change in flood magnitude, while for each point, the percentage change in flood magnitude is written into the top-right of the flood frequency curve for that point. Figure 3.4 shows how the return period of the 1000-year flood can reduce to 341 years at one point, but 533 years at another point less than 5 kilometres away.

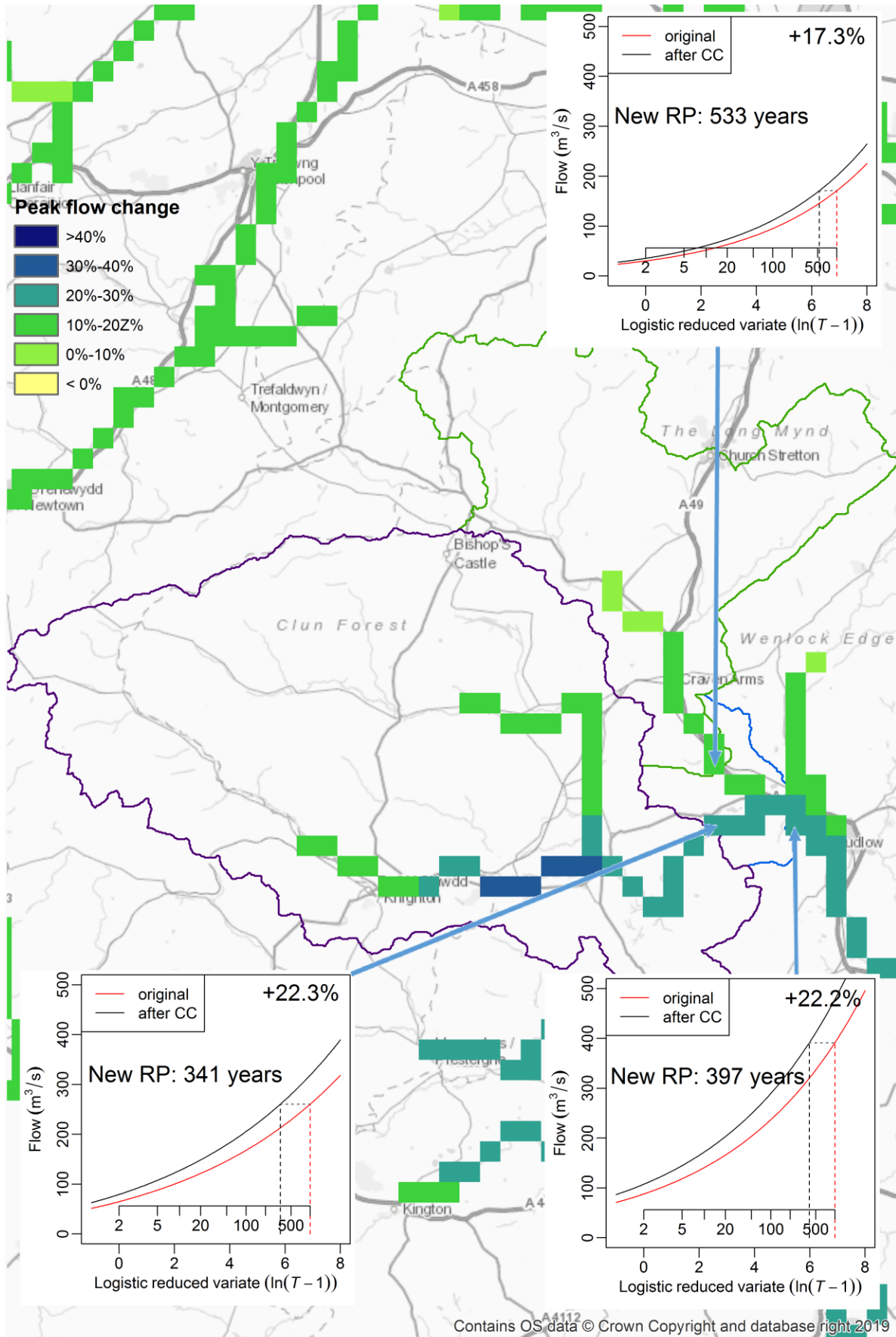


Figure 3.4 Example flood frequency plots for three nearby locations with differently shaped baseline curves, showing how the flow peak changes can give very different changes in return period, especially for the baseline 1000-year return period flood.

4 References

Bell, V.A., Kay, A.L., Jones R.G., Moore R.J. and Reynard, N.S. (2009). Use of soil data in a grid-based hydrological model to estimate spatial variation in changing flood risk across the UK. *Journal of Hydrology*, 377(3–4), 335–350.

EA (2015) Flood Estimation Guidelines. Technical guidance 197_08, Environment Agency, Bristol.

Institute of Hydrology (1999) Flood Estimation Handbook (five volumes). Centre for Ecology & Hydrology, Wallingford.

James, R., Washington, R., Schleussner, C., Rogelj, J. and Conway, D. (2017). Characterizing half-a-degree difference: a review of methods for identifying regional climate responses to global warming targets. *WIREs Climate Change*, 8:e457, doi:10.1002/wcc.457.

Kay, A.L., Crooks, S., Davies, H.N., Prudhomme, C. and Reynard, N.S. (2011). Practicalities for implementing regionalised allowances for climate change on flood flows. Report to Department for Environment, Food and Rural Affairs, Technical Report FD2648, CEH Wallingford, May 2011, 209pp.

Kay, A.L., Crooks, S.M., Davies, H.N., Prudhomme, C. and Reynard, N.S. (2014a). Probabilistic impacts of climate change on flood frequency using response surfaces. I: England and Wales. *Regional Environmental Change*, 14(3), 1215-1227, doi:10.1007/s10113-013-0563-y.

Kay, A.L., Crooks, S.M., Davies, H.N. and Reynard, N.S. (2014b). Probabilistic impacts of climate change on flood frequency using response surfaces. II: Scotland. *Regional Environmental Change*, 14(3), 1243–1255.

Kay, A.L., Rudd, A.C., Fry, M., Nash, G. (2020). Climate change and fluvial flood peaks. Report to Environment Agency, SC150009 WP2 Final Report, UKCEH, March 2020, 61pp + Appendix.

Kjeldsen, T.R., Jones, D.A. and Bayliss, A.C. (2008). Improving the FEH statistical procedures for flood frequency estimation. Joint Defra/EA Flood and Coastal Erosion Risk Management R&D Programme, Science Report SC050050, 137pp.

Met Office (2019). UKCP18 Technical Note: Clipping and Baseline advice on Land Strand 1 data in UKCP18. Met Office, March 2019.

Met Office Hadley Centre (2018). UKCP18 Probabilistic Projections by UK River Basins for 1961-2099. Centre for Environmental Data Analysis, April 2019. <http://catalogue.ceda.ac.uk/uuid/10538cf7a8d84e5e872883ea09a674f3>.

Natural Environment Research Council (1975). Flood Studies Report (five volumes). NERC, London.

Prudhomme, C., Wilby, R.L., Crooks, S., Kay, A.L. and Reynard, N.S. (2010). Scenario-neutral approach to climate change impact studies: Application to flood risk. *Journal of Hydrology*, 390, 198-209, doi:10.1016/j.jhydrol.2010.06.043.

Prudhomme, C., Crooks S., Kay, A.L. and Reynard, N.S. (2013). Climate change and river flooding: Part 1 Classifying the sensitivity of British catchments. *Climatic Change*, 119(3-4), 933-948, doi:10.1007/s10584-013-0748-x.

Reed, D. W. (1999). Overview. Volume 1 of the Flood Estimation Handbook. Centre for Ecology & Hydrology, Wallingford.

Reynard, N.S., Crooks, S., Kay, A.L. and Prudhomme, C. (2009). Regionalised impacts of climate change on flood flows. Report to Department for Environment, Food and Rural Affairs, Technical Report FD2020, CEH Wallingford, November 2009, 113pp.



BANGOR

UK Centre for Ecology & Hydrology
Environment Centre Wales
Deiniol Road
Bangor
Gwynedd
LL57 2UW
United Kingdom
T: +44 (0)1248 374500
F: +44 (0)1248 362133

EDINBURGH

UK Centre for Ecology & Hydrology
Bush Estate
Penicuik
Midlothian
EH26 0QB
United Kingdom
T: +44 (0)131 4454343
F: +44 (0)131 4453943

LANCASTER

UK Centre for Ecology & Hydrology
Lancaster Environment Centre
Library Avenue
Bailrigg
Lancaster
LA1 4AP
United Kingdom
T: +44 (0)1524 595800
F: +44 (0)1524 61536

WALLINGFORD (Headquarters)

UK Centre for Ecology & Hydrology
Maclean Building
Benson Lane
Crowmarsh Gifford
Wallingford
Oxfordshire
OX10 8BB
United Kingdom
T: +44 (0)1491 838800
F: +44 (0)1491 692424

enquiries@ceh.ac.uk

www.ceh.ac.uk